Revisiting the Kinetics and Mechanism of Glycerol Hydrochlorination in the Presence of Homogeneous Catalysts

Medina, Ananias; Ibáñez Abad, Javier ; Tolvanen, Pasi; De Araujo, Cesar; Salmi, Tapio

Published in:
Industrial & Engineering Chemistry Research

DOI:
10.1021/acs.iecr.2c01805

Published: 21/09/2022

Document Version
Final published version

I&EC research
Industrial & Engineering Chemistry Research

pubs.acs.org/IECR

Article

Revisiting the Kinetics and Mechanism of Glycerol Hydrochlorination in the Presence of Homogeneous Catalysts

Ananias Medina, Javier Ibáñez Abad, Pasi Tolvanen, Cesar de Araujo Filho, and Tapio Salmi*

Cite This: *Ind. Eng. Chem. Res.* 2022, 61, 13827−13840

Read Online

ACCESS | Metrics & More | Article Recommendations | Supporting Information

ABSTRACT: Recent studies have provided new information on glycerol hydrochlorination in the presence of carboxylic acids as homogeneous catalysts; particularly interesting is the fact that a part of the carboxylic acid is esterified in some of the steps in the reaction mechanism. Inspired by this observation and the previously proposed mechanism for glycerol hydrochlorination, new kinetic equations were derived. By using the quasi-equilibrium approximation for the reaction intermediates, the rate equations take into account the fraction of catalyst that is present in the form of esters and epoxides. The model explains the initial zero-order kinetics with respect to glycerol. The parameters of the new kinetic equations were fitted by non-linear regression for the set of ordinary differential equations describing the mass balances of the system. Internal control variables were the experimentally recorded temperature inside the reactor and the measured hydrogen chloride concentration in the liquid phase. The kinetic model was fitted to experimental data, and it was confirmed that the rate equations are able to describe the concentration profiles under various conditions. Incorporation of the activity coefficient of hydrogen chloride improved slightly the model predictions. The new kinetic model reduces to the previously proposed kinetic model at carboxylic acid concentrations.

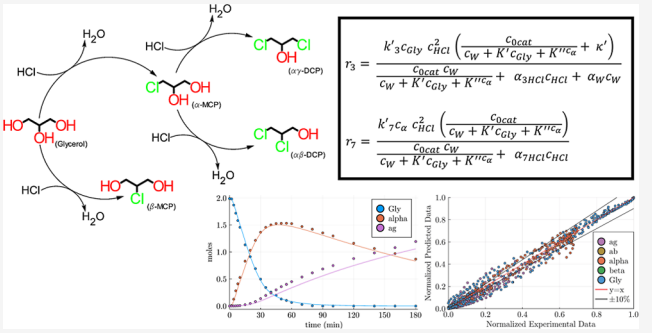

1. INTRODUCTION

Glycerol is a popular raw material because huge stoichiometric amounts of glycerol appear in the production of fatty acid methyl esters (FAMEs) through transesterification of triglycerides. From one triglyceride molecule, three molecules of fatty acid methyl esters and one molecule of glycerol are inevitably formed.[1−4]

Burning of glycerol is always an option to obtain heat, but several characteristics of glycerol, such as high viscosity and a low energy density, imply that this process has a low added value.[5,6] Therefore, during the recent years, the scientific community has focused on the valorization of glycerol by chemical transformations. Several industrially very important molecules can be obtained from glycerol, provided that active and selective catalysts are available and the reaction conditions can be optimized. Typical potential products from glycerol are acrolein, propylene glycol, diols, ethers, carbonates, glycidol, and epichlorydrin.[7−14] Also, the use of glycerol for hydrogen production has been investigated.[15,16] Epichlorohydrin can be obtained from hydrochlorinated products of glycerol.[17−22] Hydrochlorination of glycerol with HCl in the presence of carboxylic acids, such as acetic acid, propionic acid, and adipic acid, is a proven concept,[20] which leads to 3-chloro-1,2-propanediol (α-MCP), 2-chloro-1,3-propanediol (β-MCP), 1,3-dichloro-2-propanol ($\alpha\gamma$-DCP), and 1,2-dichloro-3-propanol ($\alpha\beta$-DCP), as displayed in Figure 1. The final product $\alpha\gamma$-DCP is particularly useful because it is able to react with alkali (NaOH and KOH) giving 1-chloro-2,3-epoxypropane (epichlorohydrin) as the product.[17−23] Epichlorohydrin is used extensively by chemical industry to produce epoxy resins and plasticizers. Compared to the traditional pathway for epichlorohydrin manufacture, halogenation of propene, the hydrochlorination process is a greener alternative because a high selectivity of $\alpha\gamma$-DCP is achieved and the appearance of stoichiometric co-products is avoided.[19,20]

For a chemical process, the reaction thermodynamics and kinetics are of crucial importance. The thermodynamic equilibria of the glycerol hydrochlorination process are strongly shifted to the side of the reaction products, and typically, the final hydrochlorination steps in the reaction mechanism are regarded as irreversible. The reaction mechanism and kinetics of glycerol hydrochlorination are still a matter of debate, and controversial information appears in the literature. Tesser et al.[23] reported a very complete study on the reaction mechanism for the hydrochlorination of glycerol, and the approach was extended by de Araujo Filho et

Received: May 25, 2022
Revised: August 14, 2022
Accepted: August 20, 2022
Published: September 6, 2022

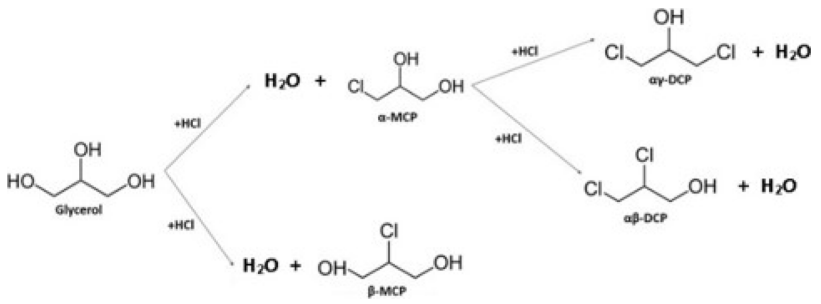

Figure 1. Reaction scheme for glycerol hydrochlorination in the presence of a homogeneous catalyst.

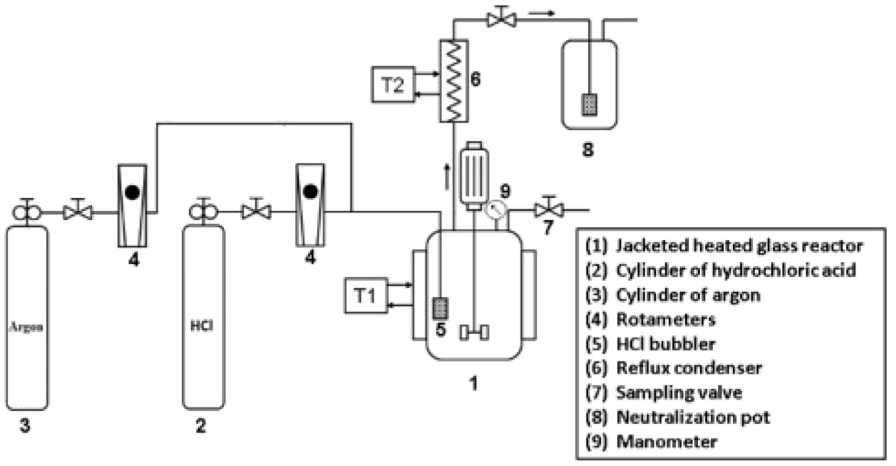

Figure 2. Overview of the semibatch glycerol hydrochlorination equipment.

al.,[24,25] who confirmed a parallel non-catalytic hydrochlorination pathway, which has an important effect on the reaction kinetics at elevated temperatures. According the current view on the glycerol hydrochlorination, the formation of esters from glycerol and the homogeneous acid catalyst is one of the key steps in the reaction mechanism. Recent information has been published by Medina et al.,[26] corroborating the previous findings and focusing on the development of a new method based on gas chromatography to quantify the ester intermediates present in the reaction system. The new findings reported in their work[26] were the behavior of the ester concentrations and the temperature changes during the reaction.

Based on these new information available, we decided to interpret the experimental data provided by Medina et al.[26] with a new kinetic model for glycerol hydrochlorination, which is presented in this work as an extension of the model published previously by de Araujo Filho et al.[24,25]

2. EXPERIMENTAL EQUIPMENT AND PROCEDURES

Experimental data and procedures are explained in detail in a previous publication of Medina et al.,[26] so in this section, a brief summary is presented. A jacketed glass vessel of 250 mL was used as the semibatch reactor. Gaseous hydrogen chloride (HCl) and liquid glycerol were used as reactants, and acetic acid was used as the homogeneous catalyst. A condenser was attached to the reactor vessel to prevent the evaporation of volatile species at high temperatures but allowing the escape of HCl. The unreacted HCl, which passed the condenser, was neutralized in a bottle containing NaOH. Figure 2 depicts an overview of the reactor setup used.

Acetic acid and glycerol were added to the reactor and heated up until the desired reaction temperature was achieved. The stirring rate was adjusted so that the gas−liquid mass-transfer resistance was suppressed, following the concept of de Araujo Filho et al.[25] The reaction was started at the moment the HCl gas valve was opened. Samples were withdrawn from the liquid phase during the course of the reaction, and they were suddenly quenched to stop the reaction for further chemical analysis. The samples were analyzed by two different methods, titration with alkali to determine the content of dissolved HCl in the sample and capillary gas chromatography (GC) to determine the concentrations of the organic compounds in the liquid phase. The results of these analyses were converted to amounts of substance (mol) and concentrations (mol m^{-3}) by the procedures described in detail by Medina et al.[26]

3. KINETIC MODELING PRINCIPLES

3.1. Overview of the Reaction Mechanism. The reaction mechanism of glycerol hydrochlorination is displayed in Figure 3, where the presumed elementary steps in the presence of a carboxylic acid (cat) are listed. The reaction mechanism is based on the discoveries of Tesser et al.[23,27,28] and de Araujo Filho et al.[24,25] The group of Tesser et al.[23,27,28] have proposed the formation of two intermediate epoxides (I_1 and I_2), which explains the experimentally confirmed fact that the β-chlorinated product (β-MCP) is non-fertile because it is not able to form an epoxide.

Later on, Dmitriev and Zanaveskin[29] reported that hydrochlorination can progress even in the absence of an added homogeneous catalyst. They[29] did however not proceed to kinetic modeling based on molecular reaction mechanisms. De

https://doi.org/10.1021/acs.iecr.2c01805
Ind. Eng. Chem. Res. 2022, 61, 13827−13840

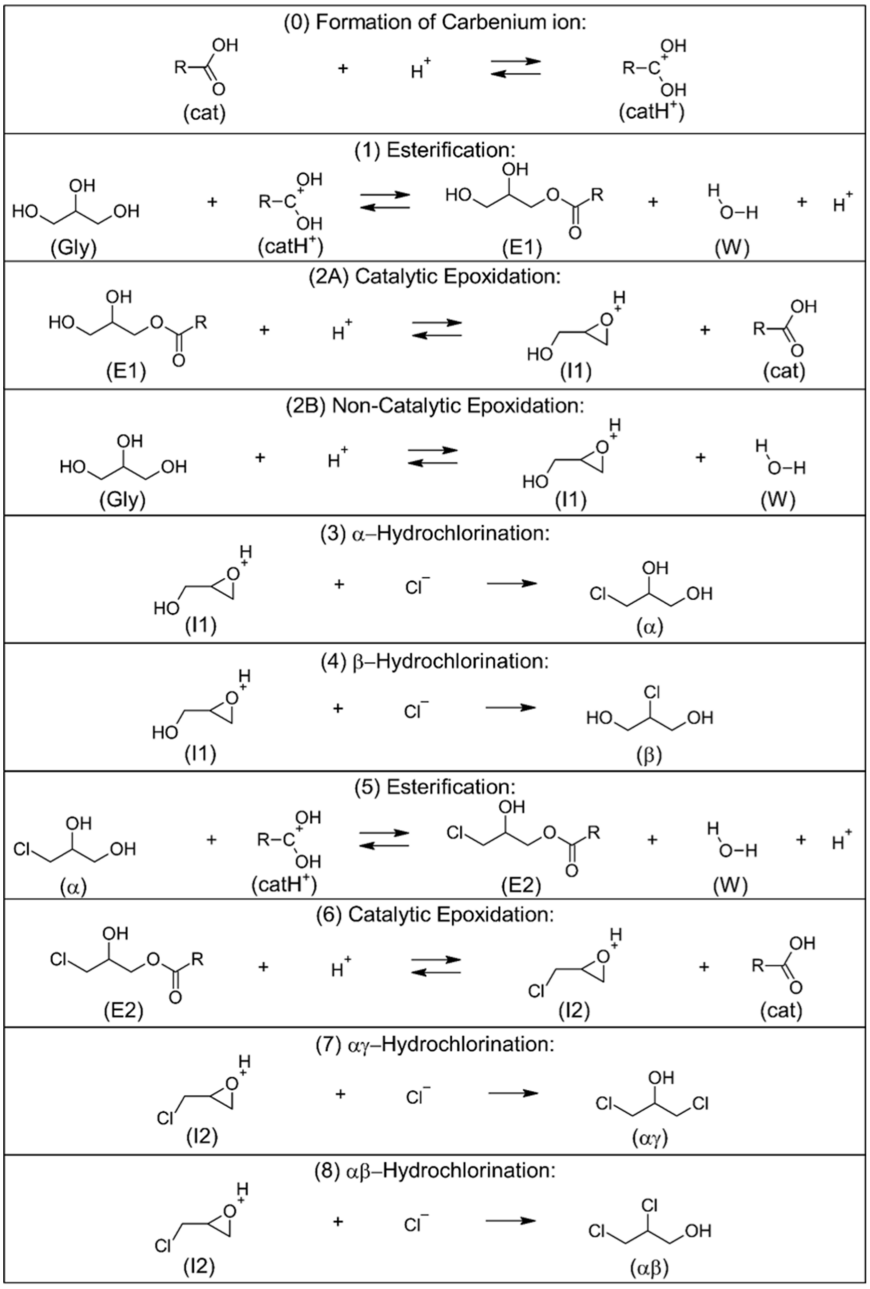

Figure 3. Reaction steps in glycerol hydrochlorination.

Araujo Filho et al.[25] confirmed the non-catalytic route by experiments conducted in a semibatch reactor and proposed the reaction step 2B in the scheme displayed in Figure 3. The role of the non-catalytic pathway in the formation of the $\alpha\gamma$-DCP and $\alpha\beta$-DCP dichlorinated products was found to be negligible based on experimental evidence. Therefore, the non-catalytic step 6B corresponding to step 2B is not included in Figure 3 ($\alpha + H^+ = I_2^+ + W$).

A detailed analysis of the reaction routes and stoichiometric numbers is provided in a previous article of de Araujo Filho et al.[25] and is thus not repeated here. Steps (0−8) give the overall reactions displayed in Figure 3, that is, the formation stoichiometry of the hydrochlorinated products

$$\mathrm{Gly} + \mathrm{H^+Cl^-} \rightarrow \alpha + \mathrm{W}$$

$$\mathrm{Gly} + \mathrm{H^+Cl^-} \rightarrow \beta + \mathrm{W}$$

$$\alpha + \mathrm{H^+Cl^-} \rightarrow \alpha\gamma + \mathrm{W}$$

$$\alpha + \mathrm{H^+Cl^-} \rightarrow \alpha\beta + \mathrm{W}$$

where Gly = glycerol, W = water, α = 3-chloro-1,2-propanediol (α-MCP), β = 2-chloro-1,3-propanediol (β-MCP), $\alpha\gamma$ = 1,3-dichloro-2-propanol ($\alpha\gamma$-DCP), and $\alpha\beta$ = 1,2-dichloro-3-propanol ($\alpha\beta$-DCP) (see Figure 1). The chlorination steps are assumed irreversible, while the other steps in the mechanism are considered as reversible in the sequel.

In the previous work of our group, the quasi-steady-state hypothesis was applied on the reaction intermediates, that is, esters E_1 and E_2 as well as epoxides I_1 and I_2. In general, the justification of the quasi-steady-state approximation is based on the hypothesis that the concentrations of the intermediates are low. This is certainly true for epoxides I_1 and I_2 and the carbenium ions $catH^+$ appearing in the mechanism (Figure 3)

https://doi.org/10.1021/acs.iecr.2c01805
Ind. Eng. Chem. Res. 2022, 61, 13827−13840

but not necessarily true for neutral intermediates E_1 and E_2, the stabilities of which can be confirmed by chemical analysis.[26] It is very well known since the pioneering work of Berthelot et Saint-Gilles[30] that the carboxylic acids form esters and that the process is acid-catalyzed. Both organic and inorganic acids can be used as catalysts for the esterification of carboxylic acids. Nowadays, efficient and intensified esterification processes are carried out in large scale with the aid of solid acid catalysts, such as cation-exchange resins, which are active, stable, and inexpensive.[31−38]

The rate equations proposed previously by de Araujo Filho et al.[25] will be revisited and generalized, taking into account the fact that a part of acetic acid can be bound to the ester (E_1 and E_2) intermediates. The formation of the esters in steps 1 and 5 (Figure 3) is presumed to be rapid compared to the hydrochlorination steps, so the quasi-equilibrium hypothesis can be applied on these steps.

3.2. Derivation of Rate Equations. The total molar balance for the added acid catalyst can be written as (Figure 3)

$$c_{\mathrm{cat0}} = c_{\mathrm{cat}} + c_{\mathrm{catH^+}} + c_{\mathrm{E_1}} + c_{\mathrm{E_2}} \tag{1}$$

In the previous work of de Araujo Filho *et al.*,[24,25] the concentrations $c_{\mathrm{catH^{+-}}}$, c, and c were approximated to be negligible in the total balance of the catalyst. The concentration of the carbenium ion $c_{\mathrm{catH^+}}$ is certainly very low because it cannot be detected by conventional analysis, such as gas chromatography or NMR. However, recently, Medina et al.[26] detected experimentally the esters because high initial concentrations of acetic acid were used in their hydrochlorination experiments. Therefore, the new approach described in the previous section is justified. The quasi-steady-state hypothesis is applied on the ionic intermediates (I_1 and I_2) but not any more on the esters (E_1 and E_2). For epoxide I_1, the quasi-steady-state approximation implies according to Figure 3

$$r_{\mathrm{I_1}} = r_{2\mathrm{A}} + r_{2\mathrm{B}} - r_3 - r_4 = 0 \tag{2}$$

which in fact means that [the merged parameters ($a_{2\mathrm{A}}$, $a_{-2\mathrm{A}}$, etc.) are explained in notation]

$$a_{2\mathrm{A}} - a_{-2\mathrm{A}}c_{\mathrm{I_1}} + a_{2\mathrm{B}} - a_{-2\mathrm{B}}c_{\mathrm{I_1}} - a_3c_{\mathrm{I_1}} - a_4c_{\mathrm{I_1}} = 0 \tag{3}$$

from which the concentration of I_1 is easily solved

$$c_{\mathrm{I_1}} = \frac{a_{2\mathrm{A}} + a_{2\mathrm{B}}}{a_{-2\mathrm{A}} + a_{-2\mathrm{B}} + a_3 + a_4} \tag{4}$$

The rate of the irreversible step 3 giving the α-hydrochlorinated compound is

$$r_3 = k_3c_{\mathrm{Cl}}c_{\mathrm{I_1}} \tag{5}$$

After inserting the expression for I_1, eq 4, and recalling the original parameters, the rate equation becomes

$$r_3 = \frac{k_3(k_{2\mathrm{A}}c_{\mathrm{E_1}} + k_{2\mathrm{B}}c_{\mathrm{Gly}})\, c_{\mathrm{H}}\, c_{\mathrm{Cl}}}{k_{-2\mathrm{A}}c_{\mathrm{cat}} + k_{-2\mathrm{B}}c_{\mathrm{W}} + (k_3 + k_4)c_{\mathrm{Cl}}} \tag{6}$$

The dominating source of protons in the solution is HCl, which as a strong acid can be regarded as fully dissociated. Thus, it is reasonable to presume that $c_{\mathrm{H}} = c_{\mathrm{Cl}} = c_{\mathrm{HCl}}$ because HCl is a much stronger acid than acetic acid. Now, the rate equation obtains the form

$$r_3 = \frac{k_3\,(k_{2\mathrm{A}}c_{\mathrm{E_1}} + k_{2\mathrm{B}}c_{\mathrm{Gly}})\, c_{\mathrm{HCl}}^{\,2}}{k_{-2\mathrm{A}}c_{\mathrm{cat}} + k_{-2\mathrm{B}}c_{\mathrm{W}} + (k_3 + k_4)c_{\mathrm{HCl}}} \tag{7}$$

The derivation of the rate equation for step 7 is not repeated here because it is completely analogous. The non-catalytic step for the formation of the epoxide intermediate (I_2) is excluded, and we get

$$r_7 = \frac{k_7(k_6c_{\mathrm{E_2}})c_{\mathrm{HCl}}^{\,2}}{k_{-6}c_{\mathrm{cat}} + (k_7 + k_8)c_{\mathrm{HCl}}} \tag{8}$$

Provided that the formation of the intermediate ($\mathrm{cat_{H^+}}$) as well as of both esters (E_1 and E_2) can be regarded as rapid compared to the hydrochlorination steps, the quasi-equilibrium hypothesis can be applied to steps 0 and 1 as well as steps 0 and 5. By taking the merged products K_0K_1 and K_0K_5, we obtain

$$K_0K_1 = K' = \frac{c_{\mathrm{E_1}}\, c_{\mathrm{W}}}{c_{\mathrm{Gly}}c_{\mathrm{cat}}} \tag{9}$$

$$K_0K_5 = K'' = \frac{c_{\mathrm{E_1}}\, c_{\mathrm{W}}}{c_{\alpha}c_{\mathrm{cat}}} \tag{10}$$

from which the concentrations of E_1 and E_2 are solved

$$c_{\mathrm{E_1}} = \frac{K_0K_1c_{\mathrm{Gly}}c_{\mathrm{cat}}}{c_{\mathrm{W}}} \tag{11}$$

$$c_{\mathrm{E_2}} = \frac{K_0K_5c_{\alpha}c_{\mathrm{cat}}}{c_{\mathrm{W}}} \tag{12}$$

Recalling the total balance of the catalyst, eq 1, and inserting the expressions 11, 12 in it, the explicit expressions for E_1 and E_2 are obtained as follows (the contribution of $\mathrm{cat_{H^+}}$ to the total balance 1 is neglected)

$$c_{\mathrm{E_1}} = \frac{K_0K_1c_{\mathrm{Gly}}c_{\mathrm{0cat}}}{c_{\mathrm{W}} + K_0K_1c_{\mathrm{Gly}} + K_0K_5c_{\alpha}} \tag{13}$$

$$c_{\mathrm{E_2}} = \frac{K_0K_5c_{\alpha}c_{\mathrm{0cat}}}{c_{\mathrm{W}} + K_0K_1c_{\mathrm{Gly}} + K_0K_5c_{\alpha}} \tag{14}$$

The rate equations for steps 3 and 7 are updated by inserting the expressions 13 and 14 for the esters

$$r_3 = k_3\left(k_{2\mathrm{A}}\frac{K_0K_1c_{\mathrm{Gly}}c_{\mathrm{0cat}}}{c_{\mathrm{W}} + K_0K_1c_{\mathrm{Gly}} + K_0K_5c_{\alpha}} + k_{2\mathrm{B}}c_{\mathrm{Gly}}\right)\frac{c_{\mathrm{HCl}}^2}{D_3} \tag{15}$$

$$r_7 = k_7\left(k_6\frac{K_0K_5c_{\alpha}c_{\mathrm{0cat}}}{c_{\mathrm{W}} + K_0K_1c_{\mathrm{Gly}} + K_0K_5c_{\alpha}}\right)\frac{c_{\mathrm{HCl}}^2}{D_7} \tag{16}$$

where D_3 and D_7 are denoted below

$$D_3 = \frac{k_{-2\mathrm{A}}c_{\mathrm{0cat}}}{1 + \frac{K_0K_1c_{\mathrm{Gly}}}{c_{\mathrm{W}}} + K_0K_5c_{\alpha}/c_{\mathrm{W}}} + k_{-2\mathrm{B}}\, c_{\mathrm{W}} + (k_3 + k_4)c_{\mathrm{HCl}} \tag{17}$$

$$D_7 = \frac{k_{-6}c_{\mathrm{0cat}}}{1 + \frac{K_0K_1c_{\mathrm{Gly}}}{c_{\mathrm{W}}} + K_0K_5c_{\alpha}/c_{\mathrm{W}}} + (k_7 + k_8)\, c_{\mathrm{HCl}} \tag{18}$$

https://doi.org/10.1021/acs.iecr.2c01805
Ind. Eng. Chem. Res. 2022, 61, 13827−13840

For the estimation of the kinetic parameters, the basic parameters appearing in the rate eqs 17, 18 are merged by division of the nominators and denominators by k_{-2A} and k_{-6}, respectively. The operative forms of the rate equations become

$$r_3 = \frac{k_3' c_{Gly} c_{HCl}^2 \left(\frac{c_{0cat}}{c_W + K_{c_{Gly}}' + K'' c_\alpha} + \kappa' \right)}{\frac{c_{0cat}\, c_W}{c_W + K_{c_{Gly}}' + K'' c_\alpha} + \alpha_{3HCl} c_{HCl} + \alpha_W c_W} \quad (19)$$

$$r_7 = \frac{k_7' c_\alpha c_{HCl}^2 \left(\frac{c_{0cat}}{c_W + K' c_{Gly} + K'' c_\alpha} \right)}{\frac{c_{0cat}\, c_W}{c_W + K' c_{Gly} + K'' c_\alpha} + \alpha_{7HCl} c_{HCl}} \quad (20)$$

A separate treatment of the formation of the $\alpha\beta$-MCP and $\alpha\gamma$-MCP hydrochlorinated steps is not needed because the reaction scheme in Figure 3 reveals that $r_3/r_4 = k_3'/k_4'$ and $r_7/r_8 = k_7'/k_8'$. Consequently, the rate equations for steps 4 and 8 can be written analogously

$$r_4 = \frac{k_4' c_{Gly} c_{HCl}^2 \left(\frac{c_{0cat}}{c_W + K' c_{Gly} + K'' c_\alpha} + \kappa' \right)}{\frac{c_{0cat}\, c_W}{c_W + K' c_{Gly} + K'' c_\alpha} + \alpha_{3HCl} c_{HCl} + \alpha_W c_W} \quad (21)$$

$$r_8 = \frac{k_8' c_\alpha c_{HCl}^2 \left(\frac{c_{0cat}}{c_W + K' c_{Gly} + K'' c_\alpha} \right)}{\frac{c_{0cat}\, c_W}{c_W + K' c_{Gly} + K'' c_\alpha} + \alpha_{7HCl} c_{HCl}} \quad (22)$$

3.3. Discourse on the Rate Equations. The following discourse appears: which is the basic difference between the revisited model and the original model of de Araujo Filho et al.?[25] According to their model, the rate equation − the operative form − for step (3) is

$$r_3 = \frac{k_3' c_{Gly} c_{HCl}^2 (c_{0cat} + \kappa')}{c_{0cat} c_W + \alpha_{HCl} c_{HCl} + \alpha_W c_W} \quad (23)$$

Compared to the model of de Araujo Filho *et al.*,[25] two new parameters (K' and K'') emerge in the new model, reflecting the formation of ester intermediates E_1 and E_2. However, on the level of the overall kinetics, the impact is more profound. The model of de Araujo Filho et al.,[25] eq 23, predicts that the reaction order with respect to glycerol (Gly) is always one (1), while the new model predicts that the reaction order with respect to glycerol can be close to zero (0) in the beginning of the process. As the process is commenced, $c_W \approx 0$, $c_\alpha = 0$, and r_3 approaches the limit value, the initial rate

$$r_{30} = \frac{k_3' c_{Gly}\, c_{HCl}^2 \left(\frac{c_{0cat}}{K' c_{Gly}} + \kappa' \right)}{\alpha_{HCl} c_{HCl}} \quad (24)$$

Typically, $\kappa' \ll c_{0cat}/c_{Gly}$, which shifts the initial kinetics toward zero order with respect to glycerol (Gly). After looking carefully at the kinetic curves published previously by our group,[25,26] it might be recognized that the kinetic curves are rather straight lines in the beginning of the experiment in many cases, which gives support to the revisited model.

Concerning the effective reaction order with respect to HCl, both the new model and the previous model are identical: in the beginning of the process, the reaction is close to first order with respect to HCl but increases toward second order as water is formed in the system ($\alpha_W c_W > \alpha_{HCl} c_{HCl}$).

Table 1. Parameter Estimation Results for Esterification Equilibrium Constants K' and K''

parameter	value	RSE (%)
K'	4.2522	1.86
K''	2.2390	1.39
R^2	0.9746	

3.4. Mass Balances for the Components in the Semibatch Reactor. All the components, except unreacted gaseous HCl, were prevented to leave the reaction mixture due to the presence of the reflux condenser. Therefore, the mass balance for the organic components and water is simple

$$\frac{dn_i}{dt} = r_i V^L \quad (25)$$

where i = Gly, α-MCP, β-MCP, $\alpha\gamma$-DCP, $\alpha\beta$-DCP, and water. The generation rates of the components are obtained from the stoichiometry (Figure 3) as follows

$$r_{Gly} = -r_3 - r_4 \quad (26)$$

$$r_\alpha = r_3 - r_7 - r_8 \quad (27)$$

$$r_\beta = r_4 \quad (28)$$

$$r_{\alpha\gamma} = r_7 \quad (29)$$

$$r_{\alpha\beta} = r_8 \quad (30)$$

$$r_W = r_3 + r_4 + r_7 + r_8 \quad (31)$$

It should be recalled that the liquid-phase volume which appears in eq 25 is updated during the course of the reaction because the liquid mass and liquid volume increase considerably as the hydrochlorinated products and water are formed; accumulation of water in the system increases further the liquid mass because the presence of water improves the solubility of HCl. The updating policy introduced by de Araujo Filho et al.[25] was followed in this work.

3.5. Numerical Strategies. The mass balances 25 of the organic components were solved repeatedly during the estimation of the kinetic parameters. The backward difference method suitable for stiff ordinary differential equations (ODEs) was used, and the parameter values were adjusted by an optimization routine until the objective function

$$Q = \sum_i (y_{i\,exp,t} - y_{i,t})^2 \quad (32)$$

reached its minimum. The quality of the parameter estimation was checked with standard statistical analysis (the standard errors of the parameters), the global significance of the model, the significance of the parameters, and the degree of explanation defined as

$$R^2 = 1 - \frac{\sum (y_{i\,exp,t} - y_{i,t})^2}{\sum (y_{i\,exp,t} - y_{i,avg})^2} \quad (33)$$

where the model fit, $y_{i,t}$, is compared with the average value of the experimental data $y_{i,avg}$. As revealed by eq 33, a high value of R^2 is required to accept the modeling result, typically 0.95 or higher.

The global significances of the model and parameters were defined using the approach of Toch et al.[39]

https://doi.org/10.1021/acs.iecr.2c01805
Ind. Eng. Chem. Res. 2022, 61, 13827−13840

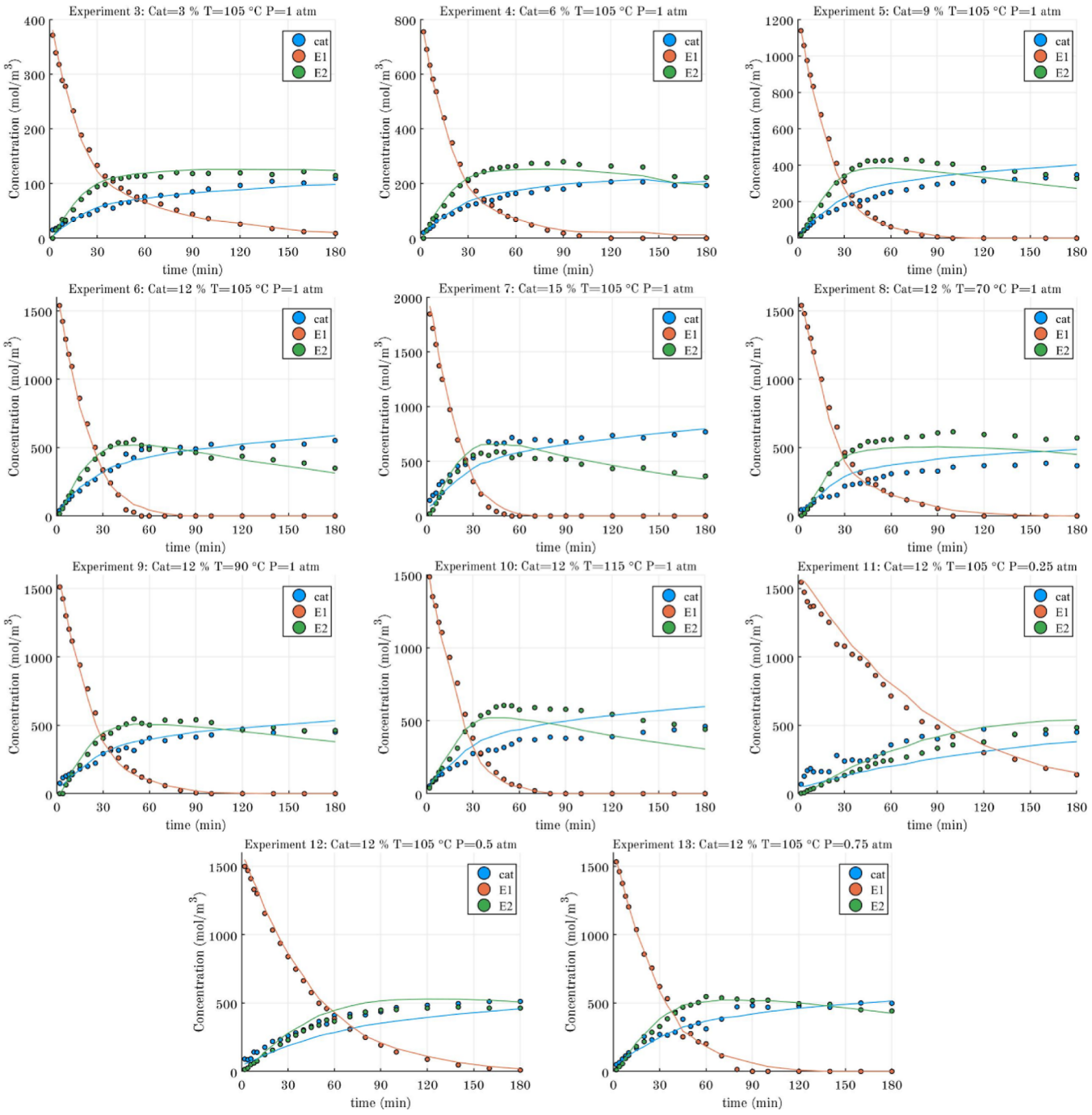

Figure 4. Concentration of intermediate esters (E_1 and E_2) and acetic acid (cat) solved in the NLAE system for esterification reactions assuming rapid equilibria.

$$F_s = \frac{\frac{\sum y_{i,t}^2}{n_p}}{\frac{\sum (y_{i\,\exp,t} - y_{i,t})^2}{n_{exp} n_{samp} n_{comp} - n_p}} \tag{34}$$

$$t(p_i) = \frac{p_i}{s(p_i)} \tag{35}$$

where F_s is the global significance of the model; $t(p_i)$ is the significance of every parameter computed as the ratio of the parameter p_i and its standard deviation $s(p_i)$; and n_{exp}, n_{samp}, n_{comp}, and n_p are the number of experiments, the number of samples per experiment, the number of analyzed chemical species per sample, and the number of parameters regressed, respectively.

The confidence intervals and standard errors were computed using the library LsqFit.jl, which is suitable to apply the Levenberg−Marquardt algorithm for optimization[40] in the programming language Julia (for details on the calculation of the covariance matrix, standard errors, and the confidence interval, visit https://julianlsolvers.github.io/LsqFit.jl/latest/tutorial/).

https://doi.org/10.1021/acs.iecr.2c01805
Ind. Eng. Chem. Res. 2022, 61, 13827−13840

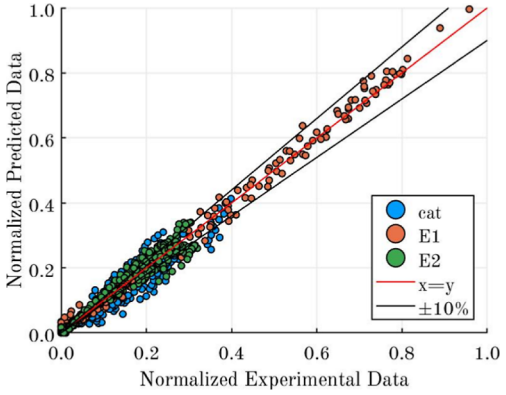

Figure 5. Parity plot for the NLAE system solved for parameter estimation of parameters K' and K''.

Several issues were taken into consideration during the parameter estimation. First, as has been demonstrated by de Araujo Filho *et al.*,[25] it is possible to model the behavior of the HCl amount in the liquid phase by the use of the double film theory. However, the errors of this prediction have a direct impact on the estimation of the kinetics parameters. For this reason, it was decided to take the HCl amount as a control variable in the parameter estimation, which allows the use of the real values calculated by titration as the moles of HCl in the system. The experimentally recorded values for HCl were introduced to the parameter estimation as a table and internally the ODE model linearly interpolated between these data. The error of the linear approximation was low due to the precise chemical analysis of HCl and the high frequency of the sampling.

The work of Medina et al.[26] revealed that the temperature inside the reactor changed considerably along the reaction as a consequence of the exothermic dissolution of the HCl gas into the liquid phase. The changes of temperature inside the reactor suggest to us that isothermal conditions should not be assumed; for this reason, the temperature data acquired during experiments were introduced as a table and the values between successive data points were interpolated.

The law of Arrhenius was used to explain the dependence of the rate constants on temperature; however, to suppress the mutual correlation between the parameters,[32] the equation was transformed by taking as the orthogonalized reciprocal temperature as the independent variable

$$z = \frac{1}{T} - \frac{1}{T_m} \tag{36}$$

where T is the temperature and T_m is in general the average of the temperatures at which the experiments had been conducted, but it can in principle be any value; the selected value during this work was T_m= 373.15 K. After the orthogonalization, the Arrhenius equation is transformed to

$$k = k_m e^{-\frac{E_a}{R}z} \tag{37}$$

where k is the rate constant, E_a is the activation energy, R is the ideal gas constant, and k_m is the rate constant at the reference temperature T_m.

The temperature dependences of the equilibrium constants, K' and K'', were discarded because esterification reactions have relatively low reaction enthalpies.[33−39] Moreover, Gelosa et al.[38] have investigated the glycerol esterification with acetic acid in the presence of a solid acid resin as the catalyst and have shown that the equilibrium constant for this reaction under the temperature range they work was virtually constant.

In the present system, the assumption of a quasi-equilibrium for the esterification reactions according to eqs 13 och 14 allows us to separate these reactions from the rest of the system and estimate the equilibrium constants as a subset of parameters in a nonlinear algebraic equation system (NLAE), that is, an algebraic model. Equations 9 and 10 give the concentrations of esters E_1 and E_2, and eqs 11 and 13 give the concentration of acetic acid

$$c_{cat} = \frac{c_W c_{0cat}}{c_W + K' c_A + K'' c_\alpha} \tag{38}$$

Since the concentrations of esters, E_1 and E_2,[26] were determined by chemical analysis, they were used to estimate the numerical values of equilibrium constants, K' and K''. The parameter estimation of the NLAE system was carried out in MATLAB applying the Levenberg−Marquardt method with the function "lsqnonlin".

The liquid phase of the current reaction system is in reality very complex with several compounds and some of them with too low amount of data available to describe their thermodynamic behavior. However, as has been explained by Medina et al.,[26] the dissociation of HCl in the solution takes place mainly in glycerol and water, and for most of the experiments, glycerol is consumed rapidly. Therefore, as an illustrative recourse, it was decided to use the mean activity coefficients for the electrolyte HCl in water calculated with the Pitzer model[41] on Aspen Plus.

4. MODELING RESULTS AND DISCUSSION

4.1. Ester Concentrations. The values of the esterification equilibrium constants, K' and K'', and their relative standard error (RSE) are shown in Table 1, and Figure 4 displays the experimental concentration of the chemical species involved in the esterification reactions under different conditions. For a visual comparison, between experimental values and predicted values, Figure 5 shows the parity plot between these data based on the results obtained by the use of eqs 13, 14, and 38. The concentration of ester E_1 decreases as the first hydrochlorination step progresses, and the ester is transformed to the α-hydrochlorinated product. The concentration of the second ester, E_2, increases first but starts to decrease as the α,γ-hydrochlorinated product appears. Finally, at high conversions of glycerol, the process stagnates and acetic acid (cat) is formed back.

The values of the parameters shown in Table 1 are in agreement with those reported by Gelosa et al.[38] and were used directly in the estimation of the other model parameters, but during the forthcoming computations, the esterification equilibrium constants were kept at fixed values.

4.2. Concentrations of Main Components. De Araujo Filho et al.[25] have shown that the parameters in the denominator of the rate expression do not have a strong temperature dependence, but the main changes of the rate constants with temperature originate from the composite parameters k_3', k_4', k_7', k_8', and κ'. Exactly the same simplification was adopted to this study. The values presented by de Araujo Filho *et al.*[25] were used as initial guesses in the estimations since the modification presented in the new model basically takes the catalyst concentration as a fraction of the initial

https://doi.org/10.1021/acs.iecr.2c01805
Ind. Eng. Chem. Res. 2022, 61, 13827−13840

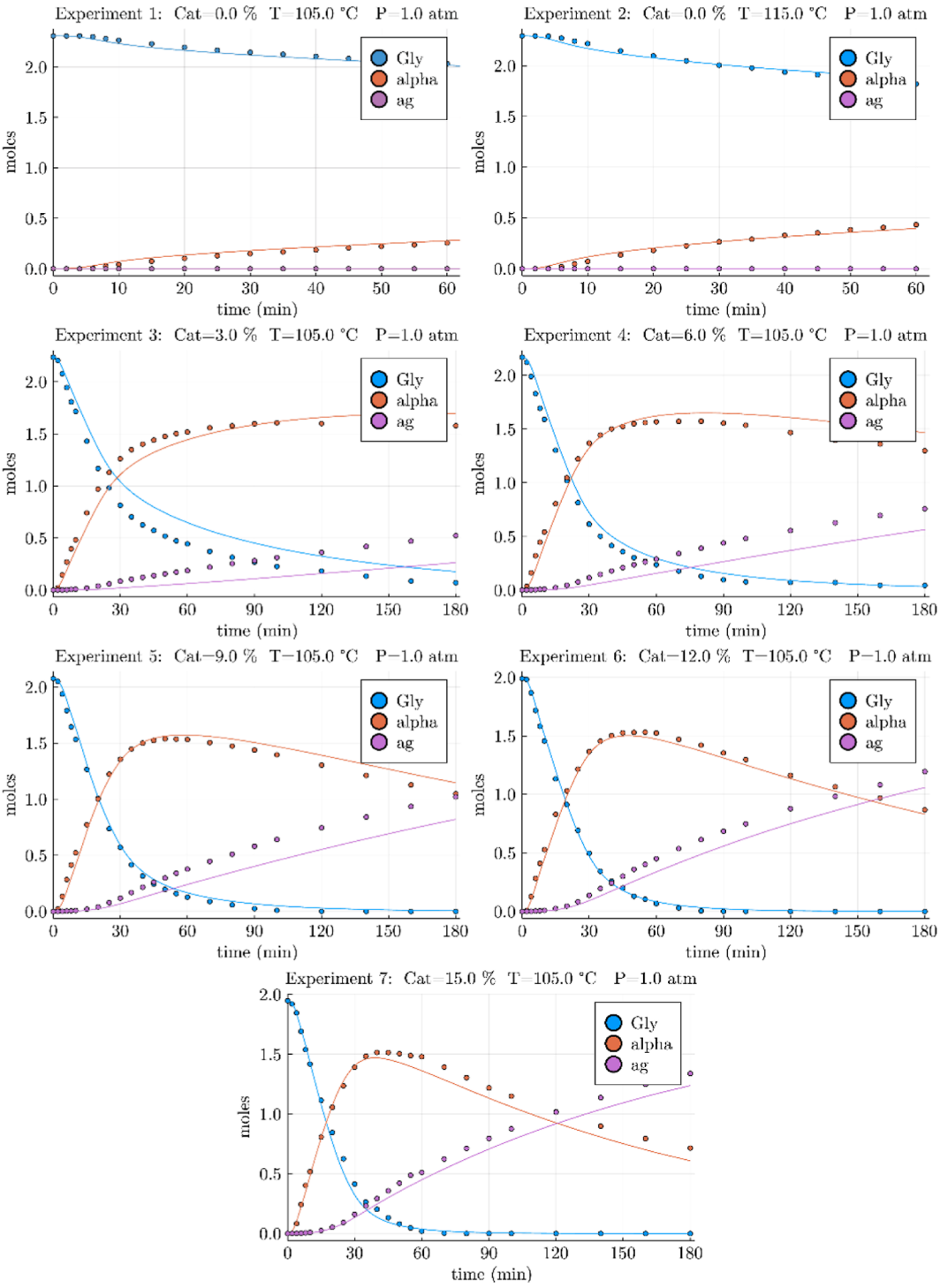

Figure 6. Fit of the kinetic model for experiments at different initial acetic acid loads, Gly = glycerol, alpha = 3-chloro-1,2-propanediol (α-MCP), and ag = 1,3-dichloro-2-propanol ($\alpha\gamma$-DCP).

amount loaded to the reactor due to the ester formation. Figures 6, 7, and 8 display the comparison between experimental data (dots) and model predictions (lines) for the 13 experiments conducted. Figure 6 shows the experimental data and model predictions for different catalyst loads; similarly, Figure 7 shows the results from the experiments conducted at different jacket temperatures, while Figure 8 displays the results from the experiments conducted at different partial pressures of HCl. The parameter values estimated by the optimization routine are collected in Tables 2 and 3; in total, 13 parameters were included, but it is important to notice that just a set of parameters was used to fit all the experimental conditions. In addition, Table 3 shows the 95% confidence interval, the RSE, and the significance of each parameter (see eq 35). The last two rows show the degree of explanation computed using eq 33 and the global significance of the model using eq 34.

The model predicts with a good accuracy the experimental trends, and just in certain conditions, the limits of the model were reached and the discrepancy between the modeled and

https://doi.org/10.1021/acs.iecr.2c01805
Ind. Eng. Chem. Res. 2022, 61, 13827−13840

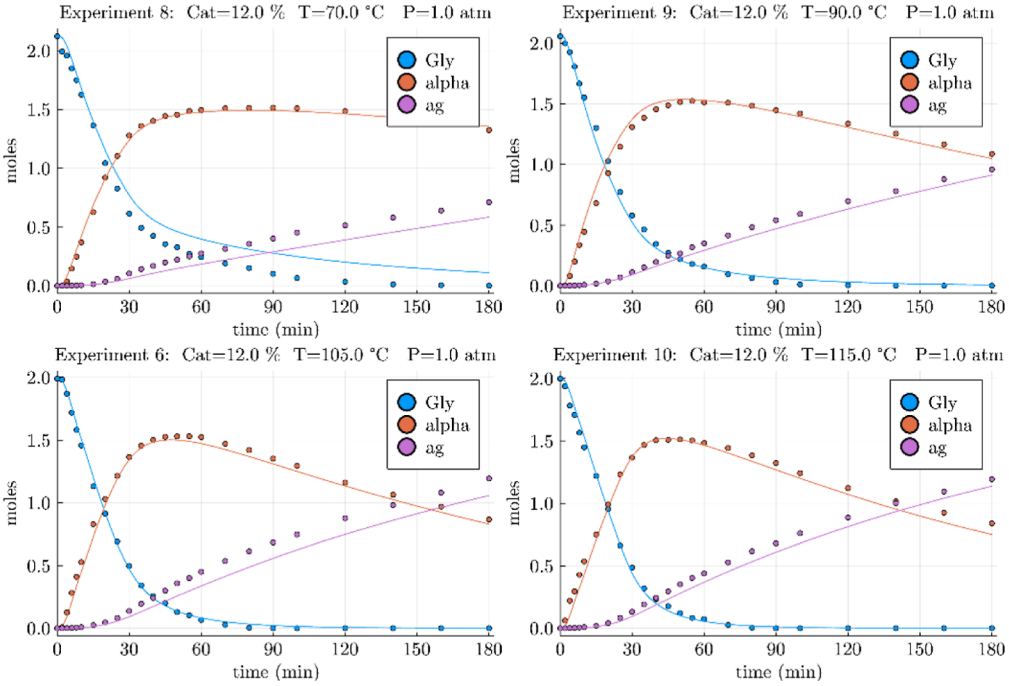

Figure 7. Fit of the kinetic model for experiments at 12 mol % of initial acetic acid load at different initial temperatures, Gly = glycerol, alpha = 3-chloro-1,2-propanediol (α-MCP), and ag = 1,3-dichloro-2-propanol ($\alpha\gamma$-DCP).

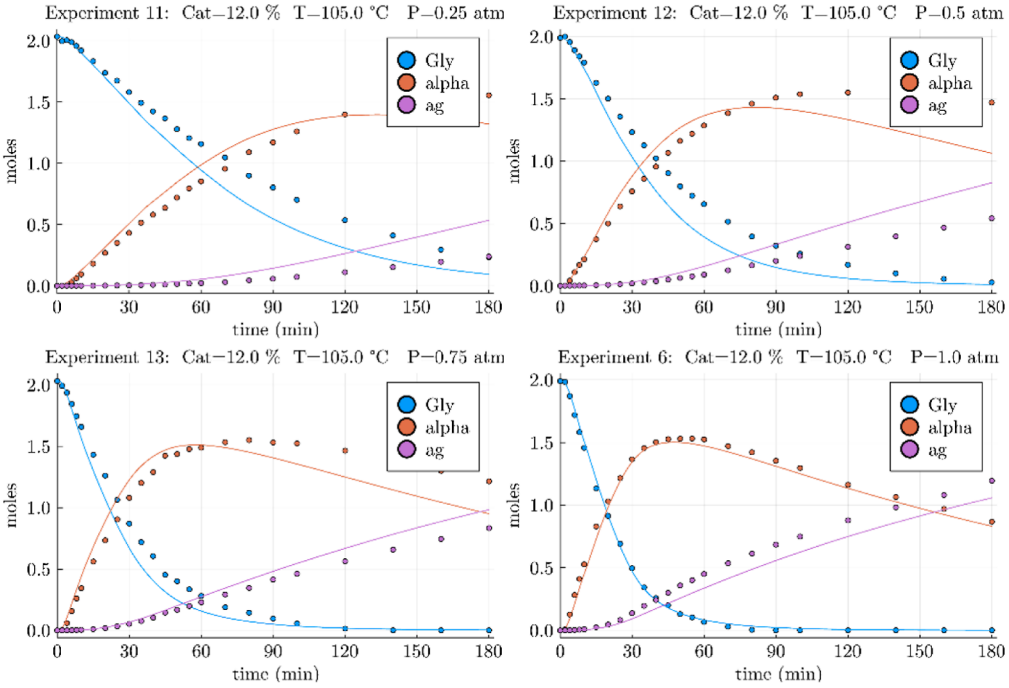

Figure 8. Fit of the kinetic model for experiments at 12 mol % of initial acetic acid load and an initial temperature of 105 °C at different partial pressures of HCl, Gly = glycerol, alpha = 3-chloro-1,2-propanediol (α-MCP), and ag = 1,3-dichloro-2-propanol ($\alpha\gamma$-DCP).

experimental amounts became visible. The main differences are observed at the lowest catalyst concentrations, at the lowest jacket temperature, and for the HCl partial pressures different from 1 atm. These differences might be explained as a deviation from ideality of the solution, probably as a consequence of the strong electrolyte HCl present in the solution. Electrolyte solutions are in general strongly non-ideal solutions; however, if the concentration of the electrolyte in solution does not change too much during experiments—which is the case for the most of our experiments—the activity coefficients can be invoked in the kinetic constants, resulting in a pseudo-ideal model. Medina et al.[26] have shown that the behavior of the HCl concentration in the solution does not change considerably compared with the experiments at the same jacket temperature and the same partial pressure; for this reason, the model gives a better prediction of these conditions where the activity coefficients for the electrolyte should behave similarly across the reaction time.

https://doi.org/10.1021/acs.iecr.2c01805
Ind. Eng. Chem. Res. 2022, 61, 13827−13840

Table 2. Estimated Parameters for Model Set 1

parameter	value	CI 95%		RSE (%)	$t(p_i)$
$k_{m,3}$	1.27572	1.27424	1.27719	0.12	864
$E_{a,3}$	76.1474	76.0933	76.2015	0.07	1408
$k_{m,4}$	0.05429	0.05379	0.05479	0.91	109
$E_{a,4}$	95.6769	95.5520	95.8017	0.13	766
$k_{m,7}$	0.16169	0.15992	0.16346	1.09	91
$E_{a,7}$	39.5976	39.5001	39.6950	0.25	406
$k_{m,8}$	0.00296	0.00218	0.00374	26.36	3
$E_{a,8}$	95.0750	94.7072	95.4428	0.39	258
α_{3HCl}	574.055	573.666	574.444	0.07	1475
α_W	1065.39	1065.39	1065.39	0.00	1.28×10^{12}
α_{7HCl}	4313.53	4296.60	4330.47	0.39	254
κ'_m	0.00040	0.00039	0.00041	2.94	33
E_a	6.01554	5.98337	6.04770	0.04	2554
R^2	0.9772				
F_s	13205				

Table 3. Estimated Parameters for Model Set 1

parameter	value	CI 95%		RSE (%)	$t(p_i)$
$k_{m,3}$	1.27572	1.27424	1.27719	0.12	864
$E_{a,3}$	76.1474	76.0933	76.2015	0.07	1408
$k_{m,4}$	0.05429	0.05379	0.05479	0.91	109
$E_{a,4}$	95.6769	95.5520	95.8017	0.13	766
$k_{m,7}$	0.16169	0.15992	0.16346	1.09	91
$E_{a,7}$	39.5976	39.5001	39.6950	0.25	406
$k_{m,8}$	0.00296	0.00218	0.00374	26.36	3
$E_{a,8}$	95.0750	94.7072	95.4428	0.39	258
α_{3HCl}	574.055	573.666	574.444	0.07	1475
α_W	1065.39	1065.39	1065.39	0.00	1.28×10^{12}
α_{7HCl}	4313.53	4296.60	4330.47	0.39	254
κ'_m	0.00040	0.00039	0.00041	2.94	33
E_a	6.01554	5.98337	6.04770	0.04	2554
R^2	0.9772				
F_s	13205				

Table 4. Estimated Parameters for Model Set 2

parameter	value	CI 95%		RSE (%)	$t(p_i)$
$k_{m,3}$	1.31574	1.31437	1.31710	0.10	964
$E_{a,3}$	71.4363	71.3994	71.4732	0.05	1937
$k_{m,4}$	0.06005	0.05901	0.06109	1.73	57
$E_{a,4}$	85.3036	85.1335	85.4738	0.20	501
$k_{m,7}$	0.16391	0.16139	0.16643	1.54	65
$E_{a,7}$	40.2159	40.0518	40.3800	0.41	245
$k_{m,8}$	0.00340	0.00268	0.00411	20.92	4
$E_{a,8}$	57.1005	56.9099	57.2911	0.33	299
α_{3HCl}	934.772	934.108	935.435	0.07	1408
α_W	747.316	747.117	747.514	0.03	3763
α_{7HCl}	3984.59	3971.09	3998.09	0.34	295
κ'_m	0.00048	0.00047	0.00049	2.04	49
E_a	12.0728	12.0118	12.1338	0.07	1369
R^2	0.9878				
F_s	18376				

4.3. Impact of the HCl Activity Coefficient. The values of the mean activity coefficients for HCl as a function of molality and temperature are shown in the Supporting Information. The maximum concentration of HCl was reached at 70 °C; at this temperature, the reaction rate is lower and the solubility of the gas is higher, and the maximum value was 3.6 mol/kg, which means that the main change in the activity is for HCl, whereas the mean activity coefficient of water (see the Supporting Information) is approximately 1 in all the experiments. The mean activity coefficient does not change appreciably with the change of catalyst load; however, for different temperatures and partial pressures, the changes are

https://doi.org/10.1021/acs.iecr.2c01805
Ind. Eng. Chem. Res. 2022, 61, 13827−13840

Table 5. Estimated Parameters for Model Set 3

parameter	value	CI 95%		RSE (%)	$t(p_i)$
$k_{m,3}$	2.40947	2.40598	2.41297	0.15	689
$E_{a,3}$	96.7595	96.7198	96.7993	0.04	2434
$k_{m,4}$	0.10100	0.10051	0.10150	0.49	205
$E_{a,4}$	116.789	116.622	116.955	0.14	701
$k_{m,7}$	0.17850	0.17701	0.17998	0.83	120
$E_{a,7}$	54.0706	54.0020	54.1392	0.13	788
$k_{m,8}$	0.00323	0.00251	0.00395	22.21	5
$E_{a,8}$	95.1516	95.0220	95.2811	0.14	734
α_{3HCl}	1098.42	1097.62	1099.22	0.07	1376
α_W	1256.71	1255.51	1257.90	0.10	1050
α_{7HCl}	3988.72	3982.88	3994.55	0.15	684
κ'_m	0.00043	0.00042	0.00044	2.05	49
E_a	−4.68943	−4.7673	−4.61146	0.08	1181
R^2	0.9837				
F_s	18627				

big enough to make a change. For different partial pressures, the mean activity coefficient decreases as the HCl partial pressure decreases, explaining why the model predicts a faster consumption of glycerol than in the experiments.

Two more sets of parameters were optimized under different conditions using same experimental data. The results are shown in Tables 4 and 5, and figures of the fitting against experimental data for these sets of parameters are presented in the Supporting Information. The first set, Model Set 2, was estimated using only the experimental data obtained with pure hydrogen chloride. This set of parameters is suitable for applications in which pure HCl gas is used. The second extra set of parameters, Model Set 3, was estimated assuming that the activity coefficient of HCl was the one computed with Aspen Plus.

4.4. Comparison of the Model Sets. As can be seen in Tables 2, 3, and 4, the models have a degree of explanation exceeding 0.95 and a global significance exceeding 100, a value suggested by Toch *et al.*[39] as the minimum value possible for a model to be reliable. Therefore, the relative standard deviation of parameters for all the models are under 30%, and as suggested by Toch et al.,[39] and the significance of most of the parameters is in or above the order of 10 to 100. For the significance of those that have low values, the result can be explained as a lack of significance in the model due to a low participation in the errors of the model, which is the case for those parameters directly involved in the reaction rates of low-concentration species like $k_{m,4}$ and $k_{m,8}$.

The results shown in Tables 3 and 4 are in agreement with those presented by de Araujo Filho et al.,[25] and the values for the activation energies are in the same order of magnitude and they mainly change due to the use of the experimental temperature, which has a strong increment at the beginning of the reaction as was shown by Medina et al.[26] For this reason, the biggest change appears in the activation energy of the rate constants for the reactions of glycerol to α-MCP and β-MCP, which are the dominating reactions at the beginning. However, the activation energies for Model Set 3 take another increase because the rate is strongly dependent on the HCl concentration/activity, which is highly modified after including the changes in the mean activity coefficient for HCl. Due to this change, the apparent activation energy E_a associated to the lumped parameter κ' becomes negative. It should be kept in mind that the evaluation of the activity coefficient includes uncertainties because the impact of organic species on the activity coefficient was not taken into account. The behavior of the activity coefficient can affect numerical values of the estimated kinetic parameters.

A comparison between the three sets of parameters can be done by observing the degree of explanation and global significance of the model, both increasing for Model Set 2 and 3. The improvement in Model Set 2 [model without the HCl activity coefficient, but one HCl partial pressure (1 atm)] endorses the fact that the model does not have the same accuracy to model the kinetics when changes in the partial pressure take place.

Concerning Model Set 3 (model with HCl activity coefficient included, all HCl partial pressures), a comparison of the global significance F_s for sets 1 and 3 reveals that the inclusion of the activity coefficient of HCl improves the model performance.

A visual comparison can be done by constructing a parity plot for each set as shown in Figure 9, where it is possible to see how in Model Set 1, although it gives a good overall fit between the model and the experimental data, some points are spread too far from the $y = x$ line. On the other hand, in the parity plot of Model Set 2, after excluding the experiments with different partial pressures, these scattered points disappear, implying that the largest deviations of the model appear when comparing with experiments at different partial pressures. For Model Set 3, the partial pressure experiments were again included, but the addition of the activity coefficient shifted the scattered points closer to the $y = x$ line, thus improving the predictions. It is clear that the assumption improves the modeling results; however, the presence of glycerol and water together should be considered in the calculation of the main activity coefficient as a possible improvement of the model.

5. CONCLUSIONS

The kinetic experiments on glycerol hydrochlorination conducted previously by our research group in a laboratory-scale semibatch reactor have revealed that considerable amounts of the homogeneous catalyst, acetic acid, are bound to glycerol esters during the progress of glycerol hydrochlorination, particularly if the initial concentration of the catalyst is high. This observation inspired us to revisit the previous kinetic model, where the esters were treated as quasi-

https://doi.org/10.1021/acs.iecr.2c01805
Ind. Eng. Chem. Res. 2022, 61, 13827−13840

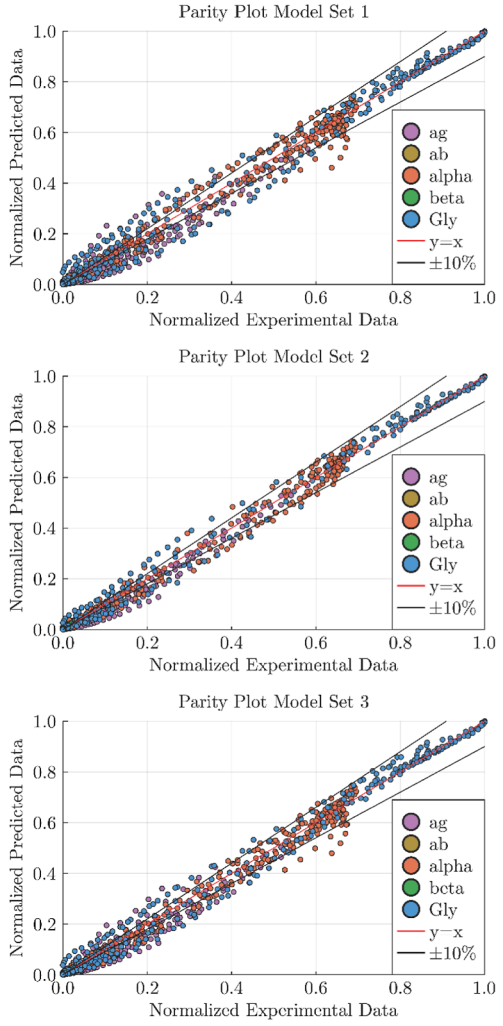

Figure 9. Parity plots for model sets 1, 2, and 3, Gly = glycerol, α = 3-chloro-1,2-propanediol (α-MCP), β = 2-chloro-1,3-propanediol (β-MCP), ag = 1,3-dichloro-2-propanol ($\alpha\gamma$-DCP), and ab = 1,2-dichloro-3-propanol ($\alpha\beta$-DCP).

steady-state intermediates. In the new kinetic model, the quasi-equilibrium hypothesis was applied on the ester formation and the total mass balance for the catalyst was reformulated. The non-ideality of the liquid phase was taken into account by including the activity coefficient of the dissolved hydrogen chloride and was presented here as a future perspective on what should be improved in the modeling of kinetics for hydrochlorination reaction. The result was a set of new rate equations for glycerol hydrochlorination. The parameters of the new model were fitted with the available experimental data, and they were able to describe the kinetic behavior of glycerol hydrochlorination reasonably well for all the experimental conditions.

■ ASSOCIATED CONTENT

Supporting Information

The Supporting Information is available free of charge at https://pubs.acs.org/doi/10.1021/acs.iecr.2c01805.

Correlation matrices and model fits for sets 1−3 and activity coefficients of HCl (PDF)

■ AUTHOR INFORMATION

Corresponding Author

Tapio Salmi − *Johan Gadolin Process Chemistry Centre (PCC), Laboratory of Industrial Chemistry and Reaction Engineering (TKR), Åbo Akademi University, Turku/Åbo FI-20500, Finland;* orcid.org/0000-0002-9271-7425; Email: tapio.salmi@abo.fi

Authors

Ananias Medina − *Johan Gadolin Process Chemistry Centre (PCC), Laboratory of Industrial Chemistry and Reaction Engineering (TKR), Åbo Akademi University, Turku/Åbo FI-20500, Finland;* orcid.org/0000-0002-7227-7645

Javier Ibáñez Abad − *Johan Gadolin Process Chemistry Centre (PCC), Laboratory of Industrial Chemistry and Reaction Engineering (TKR), Åbo Akademi University, Turku/Åbo FI-20500, Finland*

Pasi Tolvanen − *Johan Gadolin Process Chemistry Centre (PCC), Laboratory of Industrial Chemistry and Reaction Engineering (TKR), Åbo Akademi University, Turku/Åbo FI-20500, Finland;* orcid.org/0000-0003-0462-1421

Cesar de Araujo Filho − *Johan Gadolin Process Chemistry Centre (PCC), Laboratory of Industrial Chemistry and Reaction Engineering (TKR), Åbo Akademi University, Turku/Åbo FI-20500, Finland*

Complete contact information is available at: https://pubs.acs.org/10.1021/acs.iecr.2c01805

Funding

This work is part of the activities financed by the Academy of Finland, the Academy Professor grants 319002, 320115, and 345053 (Tapio Salmi and Ananias Medina). The economic support from Magnus Ehrnrooth Foundation is gratefully acknowledged (Ananias Medina).

Notes

The authors declare no competing financial interest.

■ NOMENCLATURE

a	merged constant in the derivation of rate equations
c	concentration [mol m^{-3}]
D	denominator in rate eqs [17, 18]
E_a	activation energy [kJ mol^{-1}]
k,k'	reaction rate parameter (depends on kinetics)
K	equilibrium constant (depends on stoichiometry)
K',K''	equilibrium parameters for ester formation [-]
k_m	pre-exponential factor (depends on rate equation)
n	amount of substance [mol]
P	pressure [atm]
Q	objective function [mol^2]
r	reaction rate [mol m^{-3} min^{-1}]
R	ideal gas constant [8.3143 J mol^{-1} K^{-1}]
R^2	degree of explanation [-]
t	time [min]
T	temperature [K]
V	volume [m^3]
z	reciprocal absolute temperature [K]
α	merged rate parameter
κ'	merged rate parameter

■ SUBSCRIPTS AND SUPERSCRIPTS

avg	average value
cat	catalyst

i	component index
L	liquid phase
0	initial condition
exp	experimental value

MERGED PARAMETERS

a_{2A}	$k_{2A}c_{E1}c_H$
a_{-2A}	$k_{-2A}c_{cat}$
a_{2B}	$k_{2B}c_Ac_H$
a_{-2B}	$k_{-2B}c_W$
a_3	k_3c_{Cl}
a_4	k_4c_{Cl}
k_3'	$k_3k_{2A}K'/k_{-2A}$
k_4'	$k_4k_{2A}K'/k_{-2A}$
k_7'	k_7k_6K'/k_{-6}
k_8'	k_8k_6K'/k_{-6}
α_W	k_{-2B}/k_{-2A}
α_3	$k_3 + k_4/k_{-2A}$
α_7	$k_7 + k_8/k_{-6}$
κ'	$k_{2B}/k_{2A}K'$

ABBREVIATIONS

FAME	fatty acid methyl ester
Gly	glycerol
E	ester intermediate
I^+	epoxide cation intermediate
α,α-MCP	3-chloro-1,2-propanediol
β,β-MCP	2-chloro-1,3-propanediol
$\alpha\gamma,\alpha\gamma$-DCP	1,3-dichloro-2-propanol
$\alpha\beta,\alpha\beta$-DCP	1,2-dichloro-3-propanol
GC	gas chromatography
HCl	hydrogen chloride
ODEs	ordinary differential equations
NLAE	nonlinear algebraic equation
RSE	relative standard error

REFERENCES

(1) Naik, S. N.; Goud, V. V.; Rout, P. K.; Dalai, A. K. Production of First and Second Generation Biofuels: A Comprehensive Review. *Renew. Sustain. Energy Rev.* **2010**, *14*, 578−597.

(2) Leung, D. Y. C.; Wu, X.; Leung, M. K. H. A Review on Biodiesel Production Using Catalyzed Transesterification. *Appl. Energy* **2010**, *87*, 1083−1095.

(3) Tan, H. W.; Abdul Aziz, A. R.; Aroua, M. K. Glycerol Production and Its Applications as a Raw Material: A Review. *Renew. Sustain. Energy Rev.* **2013**, *27*, 118−127.

(4) McCoy, M. Glycerin Surplus. *Chem. Eng. News* **2006**, *84*, 7.

(5) Bohon, M. D.; Metzger, B. A.; Linak, W. P.; King, C. J.; Roberts, W. L. Glycerol Combustion and Emissions. *Proc. Combust. Inst.* **2011**, *33*, 2717−2724.

(6) Albarelli, J. Q.; Santos, D. T.; Holanda, M. R. Energetic and Economic Evaluation of Waste Glycerol Cogeneration in Brazil. *Braz. J. Chem. Eng.* **2011**, *28*, 691−698.

(7) Karinen, R. S.; Krause, A. O. I. New Biocomponents from Glycerol. *Appl. Catal., A* **2006**, *306*, 128−133.

(8) Pagliaro, M.; Ciriminna, R.; Kimura, H.; Rossi, M.; Della Pina, C. From Glycerol to Value-Added Products. *Angew. Chem., Int. Ed.* **2007**, *46*, 4434−4440.

(9) Zakaria, Z. Y.; Linnekoski, J.; Amin, N. A. S. Catalyst Screening for Conversion of Glycerol to Light Olefins. *Chem. Eng. J.* **2012**, *207*−*208*, 803−813.

(10) Katryniok, B.; Paul, S.; Capron, M.; Dumeignil, F. Towards the Sustainable Production of Acrolein by Glycerol Dehydration. *ChemSusChem* **2009**, *2*, 719−730.

(11) Gu, Y.; Azzouzi, A.; Pouilloux, Y.; Jérôme, F.; Barrault, J. Heterogeneously Catalyzed Etherification of Glycerol : New Pathways for Transformation of Glycerol to More Valuable Chemicals. *Green Chem.* **2008**, *10*, 164−167.

(12) Teng, W. K.; Ngoh, G. C.; Yusoff, R.; Aroua, M. K. A Review on the Performance of Glycerol Carbonate Production via Catalytic Transesterification: Effects of Influencing Parameters. *Energy Convers. Manage.* **2014**, *88*, 484−497.

(13) Markočič, E.; Kramberger, B.; van Bennekom, J. G.; Jan Heeres, H.; Vos, J.; Knez, Ž. Glycerol Reforming in Supercritical Water; a Short Review. *Renew. Sustain. Energy Rev.* **2013**, *23*, 40−48.

(14) Dasari, M. A.; Kiatsimkul, P.-P.; Sutterlin, W. R.; Suppes, G. J. Low-Pressure Hydrogenolysis of Glycerol to Propylene Glycol. *Appl. Catal., A* **2005**, *281*, 225−231.

(15) Wen, G.; Xu, Y.; Ma, H.; Xu, Z.; Tian, Z. Production of Hydrogen by Aqueous-Phase Reforming of Glycerol. *Int. J. Hydrogen Energy* **2008**, *33*, 6657−6666.

(16) Adhikari, S.; Fernando, S. D.; Haryanto, A. Hydrogen Production from Glycerol: An Update. *Energy Convers. Manage.* **2009**, *50*, 2600−2604.

(17) Carrà, S.; Santacesaria, E.; Morbidelli, M.; Schwarz, P.; Divo, C. Synthesis of Epichlorohydrin by Elimination of Hydrogen Chloride from Chlorohydrins. 1. Kinetic Aspects of the Process. *Ind. Eng. Chem. Process Des. Dev.* **1979**, *18*, 424−427.

(18) Bell, B. M.; Briggs, J. R.; Campbell, R. M.; Chambers, S. M.; Gaarenstroom, P. D.; Hippler, J. G.; Hook, B. D.; Kearns, K.; Kenney, J. M.; Kruper, W. J.; Schreck, D. J.; Theriault, C. N.; Wolfe, C. P. Glycerin as a Renewable Feedstock for Epichlorohydrin Production. The GTE Process. *Clean: Soil, Air, Water* **2008**, *36*, 657−661.

(19) Santacesaria, E.; Tesser, R.; Di Serio, M.; Casale, L.; Verde, D. New Process for Producing Epichlorohydrin via Glycerol Chlorination. *Ind. Eng. Chem. Res.* **2010**, *49*, 964−970.

(20) Santacesaria, E.; Vitiello, R.; Tesser, R.; Russo, V.; Turco, R.; Di Serio, M. Chemical and Technical Aspects of the Synthesis of Chlorohydrins from Glycerol. *Ind. Eng. Chem. Res.* **2014**, *53*, 8939−8962.

(21) Ma, L.; Zhu, J. W.; Yuan, X. Q.; Yue, Q. Synthesis of Epichlorohydrin from Dichloropropanols: Kinetic Aspects of the Process. *Chem. Eng. Res. Des.* **2007**, *85*, 1580−1585.

(22) Carrà, S.; Santacesaria, E.; Morbidelli, M.; Schwarz, P.; Divo, C. Synthesis of Epichlorohydrin by Elimination of Hydrogen Chloride from Chlorohydrins. 2. Simulation of the Reaction Unit. *Ind. Eng. Chem. Process Des. Dev.* **1979**, *18*, 428−433.

(23) Tesser, R.; Santacesaria, E.; Di Serio, M.; Di Nuzzi, G.; Fiandra, V. Kinetics of Glycerol Chlorination with Hydrochloric Acid: A New Route to α,γ-Dichlorohydrin. *Ind. Eng. Chem. Res.* **2007**, *46*, 6456−6465.

(24) de Araujo Filho, C. A.; Salmi, T.; Bernas, A.; Mikkola, J.-P. Kinetic Model for Homogeneously Catalyzed Halogenation of Glycerol. *Ind. Eng. Chem. Res.* **2013**, *52*, 1523−1530.

(25) de Araujo Filho, C. A.; Eränen, K.; Mikkola, J.-P.; Salmi, T. A Comprehensive Study on the Kinetics, Mass Transfer and Reaction Engineering Aspects of Solvent-Free Glycerol Hydrochlorination. *Chem. Eng. Sci.* **2014**, *120*, 88−104.

(26) Medina, A.; Ibáñez, J.; Tolvanen, P.; Wärnå, J.; Eränen, K.; Salmi, T. Recent Advances in the Hydrochlorination of Glycerol. *Chem. Eng. Sci.* (accepted).

(27) Tesser, R.; Di Serio, M.; Vitiello, R.; Russo, V.; Ranieri, E.; Speranza, E.; Santacesaria, E. Glycerol Chlorination in Gas−Liquid Semibatch Reactor: An Alternative Route for Chlorohydrins Production. *Ind. Eng. Chem. Res.* **2012**, *51*, 8768−8776.

(28) Vitiello, R.; Russo, V.; Turco, R.; Tesser, R.; Di Serio, M.; Santacesaria, E. Glycerol Chlorination in a Gas-Liquid Semibatch Reactor: New Catalysts for Chlorohydrin Production. *Chin. J. Catal.* **2014**, *35*, 663−669.

(29) Dmitriev, G. S.; Zanaveskin, L. Synthesis of Epichlorohydrin from Glycerol. Hydrochlorination of Glycerol. *Chem. Eng. Trans.* **2011**, *24*, 43−48.

https://doi.org/10.1021/acs.iecr.2c01805
Ind. Eng. Chem. Res. 2022, 61, 13827−13840

(30) Berthelot, M.; Saint-Gilles, L. P. Recherches sur les Affinités. De la Formation et de la Decomposition des éthers. *Ann. Chim. Phys.* **1866**, *66*, 385−422.
(31) Banchero, M.; Gozzelino, G. A Simple Pseudo-Homogeneous Reversible Kinetic Model for the Esterification of Different Fatty Acids with Methanol in the Presence of Amberlyst-15. *Energies* **2018**, *11*, 1843.
(32) Schmid, B.; Döker, M.; Gmehling, J. Esterification of Ethylene Glycol with Acetic Acid Catalyzed by Amberlyst 36. *Ind. Eng. Chem. Res.* **2008**, *47*, 698−703.
(33) Golikova, A.; Tsvetov, N.; Samarov, A.; Toikka, M.; Zvereva, I.; Trofimova, M.; Toikka, A. Excess Enthalpies and Heat of Esterification Reaction in Ethanol + Acetic Acid + Ethyl Acetate + Water System at 313.15 K. *J. Therm. Anal. Calorim.* **2020**, *139*, 1301−1307.
(34) Liu, Y.; Liu, J.; Yan, H.; Zhou, Z.; Zhou, A. Kinetic Study on Esterification of Acetic Acid with Isopropyl Alcohol Catalyzed by Ion Exchange Resin. *ACS Omega* **2019**, *4*, 19462−19468.
(35) JagadeeshBabu, P. E.; Sandesh, K.; Saidutta, M. B. Kinetics of Esterification of Acetic Acid with Methanol in the Presence of Ion Exchange Resin Catalysts. *Ind. Eng. Chem. Res.* **2011**, *50*, 7155−7160.
(36) Pöpken, T.; Götze, L.; Gmehling, J. Reaction Kinetics and Chemical Equilibrium of Homogeneously and Heterogeneously Catalyzed Acetic Acid Esterification with Methanol and Methyl Acetate Hydrolysis. *Ind. Eng. Chem. Res.* **2000**, *39*, 2601−2611.
(37) Pereira, C. S. M.; Pinho, S. P.; Silva, V. M. T. M.; Rodrigues, A. E. Thermodynamic Equilibrium and Reaction Kinetics for the Esterification of Lactic Acid with Ethanol Catalyzed by Acid Ion-Exchange Resin. *Ind. Eng. Chem. Res.* **2008**, *47*, 1453−1463.
(38) Gelosa, D.; Ramaioli, M.; Valente, G.; Morbidelli, M. Chromatographic Reactors: Esterification of Glycerol with Acetic Acid Using Acidic Polymeric Resins. *Ind. Eng. Chem. Res.* **2003**, *42*, 6536−6544.
(39) Toch, K.; Thybaut, J. W.; Marin, G. B. A Systematic Methodology for Kinetic Modeling of Chemical Reactions Applied to N-Hexane Hydroisomerization. *AIChE J.* **2015**, *61*, 880−892.
(40) Salmi, T.; Wärnå, J.; Hernández Carucci, J. R.; de Araujo Filho, C. A. *Chemical Reaction Engineering: A Computer-Aided Approach*; De Gruyter: Berlin, 2020.
(41) Pitzer, K. S.; Mayorga, G. Thermodynamics of Electrolytes. II. Activity and Osmotic Coefficients for Strong Electrolytes with One or Both Ions Univalent. *J. Phys. Chem.* **1973**, *77*, 2300−2308.

https://doi.org/10.1021/acs.iecr.2c01805
Ind. Eng. Chem. Res. 2022, 61, 13827−13840